Published in final edited form as:

Cancer Res. 2019 May 01; 79(9): 2195–2207. doi:10.1158/0008-5472.CAN-18-2133.

Combined menin and EGFR inhibitors synergize to suppress colorectal cancer via EGFR-independent and calcium-mediated repression of SKP2 transcription

Bryson W. Katona[1,2], **Rebecca A. Glynn**[2], **Kayla E. Paulosky**[2], **Zijie Feng**[2], **Caroline I. Davis**[2], **Jian Ma**[2], **Corbett T. Berry**[3,4], **Katherine M. Szigety**[2], **Smita Matkar**[2], **Yuanyuan Liu**[2], **Haoren Wang**[2], **Yuan Wu**[2,5], **Xin He**[2], **Bruce D. Freedman**[3], **Donita C. Brady**[2], **Xianxin Hua**[2]

[1]Division of Gastroenterology, University of Pennsylvania Perelman School of Medicine, Philadelphia, PA

[2]Department of Cancer Biology, Abramson Family Cancer Research Institute, University of Pennsylvania Perelman School of Medicine, Philadelphia, PA

[3]Department of Pathobiology and Biomedical Sciences, University of Pennsylvania School of Veterinary Medicine, Philadelphia, PA

[4]School of Biomedical Engineering, Science and Health Systems, Drexel University, Philadelphia, PA

[5]Department of Radiation Oncology, Hubei Cancer Hospital, Wuhan, China

Abstract

Menin is a nuclear epigenetic regulator that can both promote and suppress tumor growth in a highly tissue-specific manner. The role of menin in colorectal cancer (CRC), however, remains unclear. Here we demonstrate that menin was overexpressed in CRC and that inhibition of menin synergized with small molecule inhibitors of EGFR (iEGFR) to suppress CRC cells and tumor xenografts *in vivo* in an EGFR-independent manner. Mechanistically, menin bound the promoter of SKP2, a pro-oncogenic gene crucial for CRC growth, and promoted its expression. Moreover, the iEGFR gefitinib activated endoplasmic reticulum calcium channel inositol trisphosphate receptor 3 (IP3R3)-mediated release of calcium, which directly bound menin. Combined inhibition of menin and iEGFR-induced calcium release synergistically suppressed menin-mediated expression of SKP2 and growth of CRC. Together, these findings uncover a molecular convergence of menin and the iEGFR-induced, IP3R3-mediated calcium release on SKP2 transcription and reveal opportunities to enhance iEGFR efficacy to improve treatments for CRC.

Keywords

Colorectal cancer; menin; EGFR inhibitors; calcium signaling; SKP2

Corresponding Author: Xianxin Hua, M.D., Ph.D., Department of Cancer Biology, Abramson Family Cancer Research Institute, University of Pennsylvania, 412 BRB II/III, 421 Curie Boulevard, Philadelphia, PA 19104-6160, Phone: (215) 746-5565, Fax: (215) 746-5525, huax@pennmedicine.upenn.edu.

Conflict of interests: The authors have no conflicts of interest.

Introduction

Menin serves primarily as a nuclear scaffold protein encoded by the *MEN1* gene, and has multiple different binding partners with either positive or negative effects on gene transcription (1). Classically, menin has been considered a tumor suppressor, with pathogenic germline mutations in *MEN1* leading to multiple endocrine neoplasia type 1 (MEN1) syndrome, which predisposes affected patients to tumor formation in the pituitary, parathyroid, and pancreas (1). However, more recent data have demonstrated that menin cannot be considered a global tumor suppressor. In mixed lineage leukemia (MLL) protein fusion-induced leukemias, menin serves as a contextual tumor promoter acting as a scaffold by binding to MLL and MLL-fusion proteins through a central pocket to promote H3 lysine 4 (H3K4) histone methyltransferase activity and leukemogenesis (2). Additionally, menin acts as a tumor promoter in prostate cancer, where the menin-MLL complex serves as a critical co-activator of the androgen receptor (3). Despite these intriguingly divergent roles of menin, the precise role of this protein in other tumors, including colorectal cancer (CRC), remains unclear.

Colorectal cancer (CRC) is the third most common cause of cancer in both men and women and is one of the leading causes of cancer related mortality (4). There has been significant progress in understanding the genomics and genetics of CRC which has led to the identification of multiple common driver mutations (5), as well as consensus molecular subtypes for better characterizing these tumors (6). Gene-expression analyses have demonstrated many transcripts that are over-expressed in CRC, however, the functional relevance of these differences in protein expression is not always immediately apparent. One such protein that is over-expressed in CRC is S-phase kinase-associated protein 2 (SKP2), which is a key component of the SKP1-Cullin1-F-box (SCF) complex. SKP2 serves as an E3 ubiquitin-ligase for many important proteins that repress cell growth and cell survival, including p27 and p21 (7). SKP2 expression is very low in normal colonic mucosa, however, as pre-cancerous colonic adenomas form and then progress to CRC, SKP2 levels significantly increase (8). Furthermore, higher SKP2 levels in CRC are associated with a poorer prognosis (9).

Despite this significant progress in understanding CRC genetics and biology, survival in the setting of stage IV metastatic CRC remains less than 15%, which is in stark contrast to stage I, II, and III CRC where 5-year survival in aggregate remains over 70%, thus highlighting the need for developing better treatments for stage IV disease (10). Current chemotherapeutic regimens utilized in stage IV CRC include oxaliplatin- or irinotecan-based regimens, which are often supplemented with either a VEGF antibody or in the case of KRAS/NRAS wild type tumors, an EGFR (epidermal growth factor receptor) antibody (11).

The EGFR signaling pathway is an important driver of tumorigenesis in CRC as well as in many other tumors (12). EGFR is a transmembrane protein that after activation by EGF, leads to downstream activation of both the PI3K and MAPK pathways. EGFR signaling can be inhibited by antibodies, which target the extracellular domain, or small molecule tyrosine kinase inhibitors, which compete with ATP at the EGFR catalytic domain (12). Small molecule EGFR inhibitors (iEGFRs) have had a significant impact in the treatment of non-

small cell lung cancers with activating EGFR mutations (13). However, in metastatic CRC where there is significant upregulation of the downstream EGFR signaling pathways (5), only EGFR antibodies have demonstrated efficacy (14). Trials of iEGFRs alone in CRC have been disappointing as single agents (15,16) and when combined with other chemotherapeutic agents (17). More recently, combined use of an iEGFR and EGFR antibody showed some benefit in metastatic CRC refractory to standard chemotherapy (18), however, this combined regimen is not currently recommended as standard of care. Given the disparate results between iEGFRs and EGFR antibodies in CRC, uncovering new means to sensitize CRC cells to iEGFRs may help enhance their efficacy.

iEGFRs such as gefitinib are effective at decreasing down-stream EGFR signaling, however these small molecules also regulate non-EGFR signaling pathways within cells in an “off-target” manner (19–21). One off-target process potentially associated with gefitinib is endoplasmic reticulum (ER) stress, as shown in intestinal epithelial cells (22). As the ER is one of the largest stores of calcium within the cell, alteration of ER calcium homeostasis is one mechanism to induce ER stress. Cellular calcium levels are regulated tightly, with multiple mechanisms that preserve a calcium gradient between the low calcium concentration in the cytoplasm and the high calcium concentration in the ER (23). Calcium can be pumped from the cytoplasm into the ER via one of the three isoforms of the sarco/endoplasmic reticulum Ca^{2+}-ATPase (SERCA) (23). Conversely, calcium can also be released from the ER to the cytoplasm through calcium channels including the inositol trisphosphate receptors (IP3Rs) or the ryanodine receptors (RyRs) (23). iEGFRs gefitinib and lapatinib could increase cytosolic calcium levels by rapidly mobilizing calcium from ER stores (24), however, the role of iEGFRs and the underlying mechanism of regulation of calcium homeostasis in the colonic epithelium and in CRC remains unclear.

Herein we demonstrate that menin is over-expressed in CRC and is critical for maintenance of SKP2 expression. Furthermore, we show that the combination of menin inhibition and iEGFR-induced ER calcium release synergistically reduces SKP2 expression leading to decreased cell survival and apoptosis induction in CRC cells.

Materials and Methods

TCGA database analysis

Level 3 HiSeq RNASeq data were downloaded from the TCGA for 302 colon samples (40 normal, 262 tumor), and raw counts for each gene in each sample were extracted. Raw counts were imported into R (v3.1.1) (25), where DESeq2 (v1.4.5) (26) was applied to score genes for differential expression between tumor and normal samples. For purposes of visualization, DESeq2-calculated normalized log2-transformed counts for each sample were exported.

Flow cytometry

HT-29 pHAGE-RSV-tdTomato-2A-GCaMP6f transduced cells were seeded at a density of 2×10^6 cells per 10 cm plate and cultured for 24 hours. Cells were then treated with the indicated compounds, and after the indicated time were harvested by trypsinization. After

washing with a flow cytometry buffer composed of 1% BSA, 25 mM HEPES, 0.03% NaN_3, in PBS, cells were resuspended in this buffer and filtered. The cells were then analyzed using a BD Accuri C6 flow cytometer (BD Biosciences). The resulting data were analyzed using FlowJo software (version 10.4.1). Median FL1-H values were calculated with FlowJo and are reported as the average of three experiments +/− SD.

Calcium resin binding assays

For whole cell lysate experiments, 25 μg of HT-29 whole cell lysate was incubated with a 50% slurry (v/v) of Chelex 100 resin (Biorad), prepared with either buffer alone, 1 N NaOH, or 2 N $CaCl_2$ following the manufacturer's recommendations, and 20 mM HEPES buffer (pH 7.5) at 4°C. Upon completion of a 30-minute incubation period, all supernatant was removed from the resin by centrifugation at 5000 rpm. The remaining resin was washed three times in 20 mM HEPES buffer (pH 7.5), followed by elution of resin-bound proteins by boiling the resin in Laemmli buffer at 100°C for 10 minutes. For calcium-pulldown experiments involving recombinant menin protein, 10 ng of recombinant menin protein was bound to various charged Chelex 100 resins using the protocol above, with the slight modification of a 25 mM Tris (pH 7.5) buffer replacing the 20 mM HEPES (pH 7.5) during the resin-incubation and resin-washing steps. Western blot was then performed on the elution products as well as input.

Menin protein amplification and purification

Human menin protein with an internal deletion of an unstructured loop (resides 460–519) was cloned into a modified pET28b vector with a SUMO protein fused at the N-terminus after the His6 tag, and was then expressed in *E. coli* BL21(DE3), as described previously (27). After induction for 16 hours with 0.1 mM IPTG at 25°C, the cells were harvested by centrifugation and the pellets were resuspended in lysis buffer (50 mM Tris-HCl pH 8.0, 50 mM NaH_2PO_4, 400 mM NaCl, 3 mM imidazole, 10% glycerol, with a cocktail of protease inhibitors). Menin protein was purified through Ni-NTA agarose beads (Qiagen), as described previously (27), and used for calcium resin binding assays and for differential scanning fluorimetry.

Differential scanning fluorimetry

Differential scanning fluorimetry data were collected on a QuantStudio3TM Real-Time PCR Detection System (Applied Biosystems) at a menin protein concentration of 2 μM in either 25 mM Tris, 150 mM NaCl, pH 7.5 with or without increasing concentrations of $CaCl_2$ using SYPRO orange as described previously (28). The melting temperature was calculated by fitting the normalized data curve to the Boltzmann sigmoid equation in Prism 6 (GraphPad) as described previously (28).

Mouse xenografts

All laboratory mice were maintained on a 12-hour light-dark cycle in the animal facility at the University of Pennsylvania. All mouse experiments were approved by the University of Pennsylvania Institutional Animal Care and Use Committee and were performed in accordance with relevant institutional and national guidelines and regulations. Six-week old

NU/NU athymic female mice (strain 088) were obtained from Charles River Laboratories. HT-29 cells (2×10^6), suspended in Matrigel/PBS (1:1), were injected in the left flanks of mice. After five days, mice were distributed into four groups and treated with vehicle, gefitinib, MI-463, or gefitinib + MI-463 (N = 6 per group). A gefitinib suspension was made by suspending gefitinib in 1% Tween-80 in ddH_2O to make a 12 mg/mL suspension. Gefitinib (100 mg/kg) or vehicle (1% Tween-80 in ddH_2O) was administered daily via gavage. MI-463 was dissolved in one part DMSO and then mixed with one part PEG400 and two parts PBS. Mice were then injected with 35 mg/kg MI-463 or vehicle (DMSO, PEG400, PBS). These injections were performed daily via an intraperitoneal route for the first three days, and then changed to daily via a subcutaneous route for the remainder of the experiment. Tumor dimensions were measured with Vernier calipers every three days and tumor volume was calculated as $0.5 \times [\text{larger diameter} \times (\text{smaller diameter})^2]$. Mice were weighed every three days.

Immunohistochemistry staining

Tumors were dissected, fixed in 10% formalin at room temperature, and embedded in paraffin. Paraffin embedded sections of tumors were then deparaffinized and antigen retrieval was performed in Tris-EDTA buffer (pH 9) at 100°C for 15 minutes. After blocking for one hour at room temperature using a blocking buffer (5% goat serum, 0.05% Tween-20 in PBS), the sections were incubated with the SKP2 primary rabbit antibody overnight at 4°C. After washing three times with PBS, sections were then treated with an anti-rabbit secondary antibody (Alexa Fluor 488, #A11008, Invitrogen) and DAPI (Roche) for 1 hour at room temperature. After additional washing and mounting, the sections were then visualized using a Nikon Eclipse E800 fluorescent microscope with a CCD digital camera. To quantify staining, obtained images were analyzed using ImageJ software, measuring immunofluorescence relative to cell area. Three captured fields were analyzed for each condition with results reported as average relative fluorescence per cell area +/− SD.

Additional information regarding menin immunohistochemistry, reagents, cell culture, proliferation assays, western blotting, plasmids and transfections, RT-PCR, cell visualization assays including clonogenicity, H&E staining, live cell imaging, chromatin immunoprecipitation (ChIP) assays, and calcium resin competition assays, can be found in the Supplemental Methods section.

Results

Menin is over-expressed in CRC and provides resistance toward iEGFR-induced suppression of CRC cells

To determine if menin expression is altered in CRC, data from The Cancer Genome Atlas (TCGA) was analyzed and demonstrated that menin expression was significantly elevated in colon adenocarcinoma compared to non-cancerous colonic epithelium (Fig. 1A). Menin immunohistochemistry (IHC) on ten colon cancer samples showed increased menin expression in 70% of the colon cancer samples compared to adjacent normal colonic epithelium (Fig. 1B, 2 representative examples). Knockdown of menin with two different shRNAs in HT-29 cells (Fig. 1C) and HCT-15 cells (Supplementary Fig. S1A) led to a

minimal decrease in cell growth that was only significant for a single shRNA in HT-29 cells (Fig. 1D). Similarly, CRISPR/Cas9-mediated menin knockdown also led to only a small decrease in cell growth (Supplementary Fig. S1B). By contrast, menin over-expression (Fig. 1E) did not lead to a significant increase in cell growth in HT-29 cells (Fig. 1F). Taken together, although over-expressed, menin alone does not appear to play a major role in CRC cell growth *in vitro*. To investigate whether menin provides a survival advantage in CRC under cell stress, we tested multiple different stressors with and without menin inhibition (29) including inhibitors of EGFR (gefitinib), AKT (MK-2206), MEK (AZD-6244), IGF-1R (NVP-AEW541), and β-catenin/TCF (PKF118–310, iCRT3) as well as chemotherapeutic agents including doxorubicin, oxaliplatin, 5-FU, and irinotecan (Supplementary Fig. S1C), and found that menin was only protective against the iEGFR gefitinib. Specifically, menin knockdown by either shRNA or by sgRNA using CRISPR/Cas9 enhanced the reduction in cell growth caused by gefitinib in a dose dependent manner (Fig. 1G–H), and increased apoptosis as demonstrated by an increase in poly (ADP-ribose) polymerase (PARP) cleavage (Fig. 1I–J). These data suggest that although menin does not provide a major growth advantage in CRC cells, menin does participate in resistance to gefitinib-mediated reductions in cell growth and apoptosis induction.

As these initial studies were primarily performed with genetic manipulation of menin, it is also possible to inhibit the function of menin using targeted small molecule menin inhibitors (MIs), which can block the interaction of menin with its binding partners including MLL (29). However, whether these small molecule inhibitors effectively inhibit menin in CRC is currently unknown. To that end, we first examined MI-2–2 (29), which had no significant effect on cell growth in HT-29 cells (Supplementary Fig. S1D), but was able to effectively reduce the expression of HOXA9 (Supplementary Fig. S1E), a well validated menin target gene (2) whose expression is dependent on menin in HT-29 cells (Supplementary Fig. S1F). Other characterized MIs, MI-503 and MI-463 (30), had minimal effects on cell growth except at high concentrations (Supplementary Fig. S1G–H) and as expected they also decreased HOXA9 expression (Supplementary Fig. S1E). Similar to the genetic knockdown of menin, treatment of HT-29 cells with the combination of gefitinib and MI-2–2 significantly decreased cell growth (Fig. 2A) when compared to either gefitinib or MI-2–2 alone. This dramatic synergy was also observed via a clonogenicity assay (Supplementary Fig. S2A) and after hematoxylin and eosin (H&E) staining of HT-29 cells (Supplementary Fig. S2B). The combination of gefitinib and MI-2–2 had similar effects on other colon cancer cell lines, including HCT-15 cells (Fig. 2B) and HCT-116 cells (Supplementary Fig. S2C). This effect was also observed when other iEGFRs including lapatinib (Fig. 2C) and erlotinib (Supplementary Fig. S2D) were combined with MI-2–2 and with other MIs including MI-503 (Fig. 2D) and MI-463 (Supplementary Fig. S2E). Furthermore, combined gefitinib and MI-2–2 promoted apoptosis induction (Fig. 2E). The synergy with combined gefitinib and MI-2–2 treatment was observed in a dose dependent manner down to 10nM of MI-2–2 (Supplementary Fig. S2F–G), demonstrating the potency of the MI. Further supporting on-target effect, treatment with MI-2–2 did not inhibit cell growth after menin knockdown (Supplementary Fig. S2H). Additionally, after menin knockdown combined with gefitinib treatment, MI-2–2 did not further inhibit cell growth, and only minimally increased subsequent PARP cleavage, which is likely due to incomplete menin knockdown

(Supplementary Fig. S2H–J). Finally, to underscore the specificity of this synergy to iEGFRs, MI-2–2 was combined with chemotherapeutic agents utilized to treat colon cancer, including oxaliplatin, 5-FU, and irinotecan (Supplementary Fig. S1C), and no synergy was observed with any of these combinations suggesting a specific synergy between menin inhibition and iEGFRs.

Menin inhibition enhances the EGFR-independent suppression of CRC by iEGFRs

As there is no known direct interaction or interplay between menin and EGFR, we first investigated whether menin is involved in EGFR activation and its downstream signaling. After stimulation with EGF, menin inhibition did not inhibit phosphorylation of EGFR, AKT, or ERK (Supplementary Fig. S2K). To determine if menin inhibition sensitized cells to all forms of EGFR inhibition, HT-29 cells were treated with the EGFR antibody C225. C225 effectively inhibited EGFR phosphorylation similar to gefitinib (Fig. 2F), however, MI-2–2 did not synergistically lead to a reduction of cell growth when combined with C225 (Fig. 2G). Additionally, knockdown of EGFR with EGFR shRNAs significantly decreased phospho- and total EGFR (Fig. 2H), however, menin inhibition did not impair cell growth after EGFR knockdown (Fig. 2I). These data demonstrate that menin inhibition does not sensitize cells to inhibition of EGFR signaling, but rather likely sensitizes the CRC cells to the EGFR-independent effects of iEGFRs. To investigate the EGFR-independence of this process, the EGFR-null CRC cell line SW620 was utilized (Fig. 2J). Menin inhibition sensitized SW620 cells to gefitinib-induced growth inhibition (Fig. 2K) and apoptosis (Fig. 2L, lanes 8, 10, and 12). Expression of functional EGFR in EGFR-null SW620 cells (Supplementary Fig. S2L) had no effect on growth suppression resulting from gefitinib plus MI-2–2 (Supplementary Fig. S2M–N). Taken together, these data demonstrate that the enhancement of gefitinib-mediated suppressive effects on cells by menin inhibition occurs in an EGFR-independent manner.

Menin inhibition synergizes with gefitinib and thapsigargin, but not other inducers of ER stress

To investigate how menin inhibition synergizes with iEGFRs to repress CRC cells in an EGFR-independent manner, we sought to examine whether iEGFR-induced ER stress is involved (19–22). Gefitinib alone was found to induce ER stress in HT-29 cells as it increases CHOP expression and XBP1 splicing (Fig. 3A–B), which are both markers of ER stress. Similar results were noted in HCT-15 cells (Supplementary Fig. S3A). To determine if menin inhibition synergized with other inducers of ER stress, HT-29 cells were treated with thapsigargin (TG) (SERCA inhibitor), tunicamycin (N-linked glycosylation inhibitor), and Brefeldin-A (inhibitor of protein transport from the ER to the Golgi). Menin inhibition selectively enhanced the suppressive effects of TG (Fig. 3C), but not of other ER stressors tunicamycin (Fig. 3D) and Brefeldin-A (Fig. 3E). This selective enhancement was also noted in HCT-116 cells (Supplementary Fig. S3B), and similar to gefitinib, MI-2–2 also enhanced TG-mediated apoptosis induction (Supplementary Fig. S3C). These data illustrate the synergy between TG, which inhibits SERCAs and disrupts calcium homeostasis, and menin inhibition, thus suggesting that menin function intersects with ER-mediated calcium signaling.

Increased cytosolic calcium is important for gefitinib-mediated growth suppression

From the above findings we postulated that gefitinib and TG act via a similar mechanism to increase cytosolic calcium, which may synergize with menin inhibition to suppress CRC cells. As TG is well known to inhibit SERCAs and thus increase the cytosolic calcium concentration (31), we first determined if gefitinib and/or menin inhibition could alter cytoplasmic calcium levels. HT-29 cells expressing the genetically encoded calcium reporter GCaMP6f, which senses real time changes of calcium through fluorescence emission (32), showed no increased signal with vehicle or MI-2–2 treatment alone (Fig. 3F–G), however treatment with either gefitinib or TG substantially increased the GCaMP6f fluorescence, with or without MI-2–2 treatment (Fig. 3H–K), indicating that gefitinib, like TG, can increase cytosolic calcium levels. These results were confirmed through quantification using flow cytometry (Fig. 3L–M), further demonstrating that similar to TG, gefitinib increased cytosolic calcium in a dose dependent manner. Treatment of cells with the calcium ionophore ionomycin, to increase cytoplasmic calcium levels (33), also led to decreased cell growth (Fig. 3N) and increased apoptosis (Fig. 3O) when combined with a MI, further illustrating the importance of increased calcium in this process.

To determine if the observed calcium alterations were responsible for the synergistic cell suppression resulting from combined gefitinib and MI treatment, we treated HT-29 cells with the intracellular calcium chelator BAPTA-AM (34). BAPTA-AM alone had minimal effects on cell growth up to 5 μM (Supplementary Fig. S3D), and decreased GCaMP6f fluorescence at baseline and after gefitinib treatment (Supplementary Fig. S3E–F), consistent with cytoplasmic calcium buffering. BAPTA-AM rescued growth of HT-29 cells after gefitinib/MI-2–2 treatment (Fig. 3P), and prevented gefitinib/MI-2–2-induced apoptosis (Fig. 3Q) with a significant reduction in cleaved PARP (Supplementary Fig. S3G). A similar rescue was noted in HCT-15 cells (Supplementary Fig. S3H–I) and SW620 cells (Supplementary Fig. S3J–K). Extracellular calcium was not critical for the gefitinib/MI-2–2-mediated reduction in cell growth, as cell growth was similarly inhibited in the presence or absence of extracellular calcium, therefore supporting the role of ER calcium in this process (Supplementary Fig. S3L). Together, these results establish the importance of cytoplasmic calcium mobilization by gefitinib in gefitinib/MI-induced cell suppression. To elucidate the mechanism underlying gefitinib-induced increases in cytoplasmic calcium in CRC cells, we tested whether over-expression of SERCA2, an ER calcium pump that is specifically inhibited by TG, impacts TG-induced HT-29 cell death. Indeed, ectopic SERCA2 expression rescued cells from TG-mediated apoptosis induction and growth inhibition, whereas overexpression of SERCA2 did not rescue the cells from the growth reduction induced by co-treatment with gefitinib and MI-2–2 (Supplementary Fig. S4A–C) indicating the independence of this process from SERCA2. SERCA2 knockdown sensitized HT-29 cells to TG as expected, and also to gefitinib (Supplementary Fig. S4D–F), suggesting that gefitinib does alter ER calcium homeostasis by a SERCA2-independent mechanism.

Gefitinib activates IP3R3 to increase cytosolic calcium levels

As ER calcium is actively pumped from the cytoplasm via the SERCAs and released from the ER to the cytoplasm via the IP3Rs (23), and overexpression of SERCA2 did not provide rescue from gefitinib/MI-2–2 (Supplementary Fig. S4B–C), we examined whether IP3Rs are

involved in gefitinib/MI-2–2-mediated CRC suppression. We suppressed IP3R3 expression in HT-29 cells and found this protected cells against effects of gefitinib/MI-2–2, leading to rescued cell growth (Fig. 4A) and reduced apoptosis (Fig. 4B) with significantly decreased cleaved PARP (Fig. 4C). A similar rescue in cell growth was also observed in HCT-15 cells (Supplementary Fig. S5A–B) and SW620 cells (Supplementary Fig. S5C–D), and similarly led to reduced apoptosis (Supplementary Fig. S5E). Caffeine, which classically serves as a RYR activator, can also serve as an inhibitor of IP3R3 (35). Treatment of HT-29 cells with caffeine also led to a dose dependent rescue of cell growth in gefitinib/MI-2–2 treated cells (Fig. 4D), with similar results observed in HCT-15 (Supplementary Fig. S5F) and SW620 cells (Supplementary Fig. S5G–H), further demonstrating that IP3R3 is important for gefitinib mediated ER stress induction. Caffeine did not significantly decrease baseline cytosolic calcium levels, however consistent with inhibition of IP3R3, caffeine successfully normalized the calcium increase elicited by gefitinib on flow cytometry (Fig. 4E–F).

SKP2 transcription is influenced by intracellular calcium levels and menin

To determine how gefitinib-induced increases in cytoplasmic calcium and menin inhibition synergistically inhibit CRC cells, we examined SKP2 levels as this protein is often upregulated in CRC and is important in CRC pathogenesis (7). SKP2 levels decreased in HT-29 cells after treatment with gefitinib and MI-2–2 alone, whereas the gefitinib and MI-2–2 combination led to a further reduction in SKP2 levels and an increase in SKP2-degradation targets p27 and p21 (Fig. 5A). Similarly, higher levels of other pro-apoptotic SKP2-degradation targets FOXO1 and RBL2 (36,37) were observed after SKP reduction by gefitinib plus MI-2–2 (Supplementary Fig. S6A). The reduction in SKP2 protein level is at least partly due to transcriptional regulation, as both gefitinib and MI-2–2 alone reduced SKP2 transcript levels (Fig. 5B). Furthermore, SKP2 reduction preceded apoptosis (Fig. 5C–D), indicating that the SKP2 reduction was not induced by active apoptosis. These results were confirmed in HCT-15 cells (Supplementary Fig. S6B). Menin knockdown with shRNAs (Supplementary Fig. S6C) led to a reduction in baseline SKP2 levels, which decreased further after gefitinib treatment. The reduction in SKP2 was rescued through calcium chelation with BAPTA-AM at both the protein (Fig. 5E) and RNA levels (Supplementary Fig. S6D) which led to significantly decreased levels of cleaved PARP (Fig. 5F), and similar results were observed with caffeine (Supplementary Fig. S6E). SKP2 levels were also reduced after treatment with TG, with MI-2–2 further enhancing this reduction (Supplementary Fig. S6F). SKP2, IP3R3, and menin are all expressed, although at varying levels, in multiple colon cancer cell lines (Supplementary Fig. S6G). However, this effect on SKP2 may be specific to CRC as there was no significant SKP2 decrease observed in BON cells (Supplementary Fig. S6H), a neuroendocrine tumor cell line that is resistant to the effects of gefitinib plus MI-2–2 (Supplementary Fig. S6H–I) despite expressing menin and IP3R3 (Supplementary Fig. S6J). To confirm the relevance of SKP2 in CRC cells, HT-29 cells transduced with SKP2 shRNAs were found to be more sensitive to gefitinib, which resulted in decreased cell growth (Fig. 5G) and increased apoptosis induction (Fig. 5H). Similar effects were noted in SKP2 knockdown cells that were treated with TG (Supplementary Fig. S6K). Taken together these data illustrate the importance of SKP2 expression in CRC cells, and that menin inhibition in addition to gefitinib or TG lead to synergistic repression of CRC due to a dramatic reduction in SKP2 levels.

Menin serves as a calcium-sensing regulator of SKP2 transcriptional control

To determine how gefitinib and menin regulate *SKP2* transcription, a chromatin immunoprecipitation (ChIP) assay was performed in HT-29 cells, which revealed that menin and menin-related active histone marks (H3K4me3), catalyzed by MLL, were present at the *SKP2* promoter (Fig. 6A–B). While gefitinib did not lead to a major reduction of menin at the *SKP2* promoter, MI-2–2 reduced the level of menin at the promoter (Fig. 6A). Combined gefitinib and MI-2–2 reduced the active histone mark H3K4me3 and RNA polymerase II at the *SKP2* promoter (Fig. 6B), as well as MLL at the SKP2 promoter (Supplementary Fig. S7A), thus rationalizing the reduced *SKP2* transcript levels observed. This effect was partially reversible after calcium chelation with BAPTA-AM, which led to increased menin and increased transcriptional activity at the *SKP2* promoter (Fig. 6C–D). Similar results were obtained when examining a different region of the *SKP2* promoter (Supplementary Fig. S7B–F), thereby raising the possibility that menin's role in transcriptional control may be calcium-regulated. We therefore explored whether menin interacts directly with calcium. HT-29 cell lysate was mixed with a calcium-loaded Chelex resin, and after elution it was found that menin, similarly to the weak calcium binder PKCα (38), selectively bound to the calcium loaded resin (Fig. 6E). As a negative control MEK1, which is not a calcium binding protein, did not show any binding to the calcium-loaded resin (Fig. 6E). As menin is known to have multiple binding partners (2), to determine if this effect was specific to menin alone, an identical experiment was performed using recombinant purified menin protein, which also demonstrated that menin bound selectively to the calcium loaded resin (Fig. 6F). Additionally, calcium washes effectively competed away menin bound to calcium-loaded resin as demonstrated by the presence of menin in the flow through, whereas non-specifically bound menin was not competed away from the uncharged resin (Fig. 6G). Menin's direct binding to calcium was further confirmed using differential scanning fluorimetry (28), which showed an increase in the melting temperature of menin in the presence of $CaCl_2$, consistent with a direct interaction between menin and calcium (Fig. 6H–I).

The combination of gefitinib and a MI decrease tumor xenograft growth

To determine whether the combination of gefitinib and menin inhibition can decrease CRC cell growth *in vivo*, an experiment using HT-29 cell mouse xenografts was performed. After xenograft initiation, mice were treated with vehicle, gefitinib, MI-463, or the combination of gefitinib plus MI-463. MI-463 was used instead of MI-2–2 for the xenograft experiments given its prior efficacy *in vivo* (30). Treatment with the combination of gefitinib plus MI-463 significantly decreased tumor size (Fig. 7A), and overall mouse weight did not significantly change (Fig. 7B). Immunohistochemistry was performed on the resulting tumors, which demonstrated that while gefitinib and MI-463 alone led to only a non-significant reduction in SKP2 immunofluorescence, the combination of gefitinib and MI-2–2 significantly decreased SKP2 immunofluorescence (Fig. 7C), consistent with the prior cell culture data showing reduction in SKP2 levels. This difference in SKP2 immunofluorescence can be appreciated in representative tumor sections (Fig. 7D).

Discussion

Menin, an epigenetic regulator controlling gene expression, serves as both a tumor suppressor as well as a tumor promoter in a highly tissue-specific manner in neuroendocrine tumors, leukemia, and prostate cancer (1–3), however, little is known regarding the role of menin in the regulation of CRC. Herein we demonstrate that menin is overexpressed in CRC, and that menin is crucial for epigenetically maintaining transcription of *SKP2*, which encodes a pro-oncogenic component of the SCF complex that degrades anti-proliferative proteins (7). We show further that iEGFR-induced ER calcium release represses menin's function in promoting *SKP2* transcription and facilitates synergy with MIs to suppress CRC cells. These findings are especially significant for the following reasons: first, we demonstrate that menin directly binds the *SKP2* promoter and upregulates transcription of *SKP2* by increasing active histone modifications (H3K4m3) and RNA polymerase II, linking menin's function to epigenetic regulation of the pro-oncogenic *SKP2* gene. Second, we provide the first evidence that menin directly binds calcium and that iEGFR-induced increases in cytosolic calcium impair the ability of menin to promote *SKP2* transcription. Third, we show that iEGFRs induce calcium efflux from the ER by activating IP3R3 in an EGFR-independent manner. Finally, we illustrate that iEGFR-induced ER calcium efflux combined with menin inhibition, synergize to downregulate *SKP2* transcription and decrease CRC cell survival and tumor xenograft growth, illustrating a novel pathway of calcium signaling-mediated regulation of SKP2 expression and the importance of SKP2 expression in CRC tumorigenesis. While we cannot rule out completely that an alternative factor apart from SKP2 is mediating part of the iEGFR/MI synergy, our data does support the importance of SKP2, and together these findings uncover an important mechanism whereby menin provides critical resistance to iEGFR-induced tumor suppression in CRC by maintaining SKP2 expression.

SKP2 is a critical component of the SCF E3 ligase complex and has significant pro-tumor roles in numerous different malignancies including CRC (7,39). Our data provides the first evidence that menin promotes *SKP2* transcription through binding to the *SKP2* promoter and maintaining active histone marks. Sustaining SKP2 levels is important for CRC tumorigenesis, as we demonstrated that knockdown of SKP2 alone decreased CRC cell growth and significantly sensitized cells to iEGFRs. Therefore, targeting SKP2 expression through menin inhibition may serve as a viable therapeutic strategy in CRC, especially in the presence of iEGFRs and other molecules, such as TG, that increase ER calcium release. Given the significant role of SKP2 in cancer and the ubiquitous expression of menin, it is possible that menin may also serve as a critical regulator of *SKP2* transcription in other cancers as well. In this novel context, the combined treatment with menin inhibition and an iEGFR may also function as an effective therapeutic combination outside of CRC.

Our results also suggest that the function of menin at the *SKP2* promoter may be calcium-regulated. We showed that gefitinib increases cytosolic calcium levels, which are proportional to nuclear calcium levels (40,41), and leads to a reduction in both H3K4me3 and RNA polymerase II at the *SKP2* promoter. Consistent with the role of calcium signaling in reducing the H3K4me3 and RNA polymerase II at the *SKP2* promoter, the calcium chelator BAPTA-AM inhibited these changes. This led us to hypothesize that these increases

in cytosolic calcium induced by gefitinib may alter the transcription-activation function of menin. Therefore, using a calcium resin binding experiment we showed that menin directly binds calcium similar to other weak calcium binders such as PKCα. Further strengthening this finding, we showed that the presence of calcium significantly increased the thermal stability of menin, further supporting a direct menin-calcium interaction. These data demonstrate for the first time that calcium interacts with menin and this interaction may lead to alterations in the transcription-activation function of menin at the *SKP2* promoter. Investigating other potential menin targets that may be calcium-dependent in CRC as well as in other cancers will be an exciting next step given the diverse, tissue specific functions of menin. Furthermore, future mechanistic studies of this novel menin-calcium interaction are needed to assess whether calcium causes structural changes to menin or alters the binding and recruitment of other transcriptional activators or inhibitors.

These data also reveal novel insights about the use of iEGFRs in CRC. Unlike EGFR antibodies, iEGFRs have not shown clinical efficacy in CRC, however, they are used clinically to successfully treat other cancers (13). As with most small molecules, iEGFRs have numerous effects within cells that are separate from their intended target (19–21). While these effects may technically be referred to as “off-target” effects, the contribution of these EGFR-independent effects may be an important mechanism contributing to the anti-cancer properties of these small molecules. We demonstrate that the iEGFR gefitinib has EGFR-independent effects on CRC cells and can induce both ER stress and increases in cytoplasmic calcium levels through activation of IP3R3. These effects occur at concentrations that are higher than reported plasma levels of gefitinib (42), but are in line with intra-tumor concentrations, which can exceed 10 μM (43). These results are important for better clarifying the role of iEGFRs in ER calcium homeostasis, as much of the current evidence is conflicting. Consistent with our findings, in breast cancer cells gefitinib and lapatinib can increase cytosolic calcium levels by rapidly mobilizing calcium from ER stores (24), but in this study it is unclear what pathway mediates the calcium mobilization. Alternatively, gefitinib and erlotinib are reported to enhance the interaction between IP3R3 and select Bcl-2 family members, leading to both increased cytoplasmic calcium and resistance to apoptosis induction in lung cancer cells (44). In the current study we definitively show that iEGFRs increase cytoplasmic calcium concentrations by activating IP3R3, either directly or indirectly, to release calcium from the ER, and that inhibition of IP3R3 blocked the iEGFR-induced increase in cytosolic calcium. The detailed mechanism underlying iEGFR-induced, IP3R3-mediated calcium release remains a topic for further investigation. However, taken together these results highlight that some effects of iEGFRs are in fact EGFR-independent, and exploiting these EGFR-independent effects presents an opportunity to potentially enhance the efficacy of iEGFRs in the treatment of certain cancers.

Targeting epigenetic pathways to treat cancer is being increasingly studied, as evidenced by the multiple ongoing clinical trials examining the use of histone deacetylase (HDAC) inhibitors in combination with other agents, including iEGFRs, for the treatment of a variety of different malignancies (45–47). Our data demonstrate that MIs may serve as an effective epigenetic therapy to sensitize CRC to iEGFRs. We show the effects of this synergy in CRC cell lines with differing *KRAS, BRAF*, and *TP53* mutation status, suggesting that this

synergy does not depend on some of the common genetic alterations observed in CRC. Additionally, this synergy is observed with multiple different iEGFRs, and with multiple methods of menin inhibition including small molecules as well as menin knockdown. We further extended the benefits of using MIs to sensitize CRC cells to iEGFRs to an *in vivo* xenograft experiment, where the combination treatment produced significant suppression of CRC xenografts. These results have particular relevance given the clinical ineffectiveness of both iEGFRs in CRC and of EGFR antibodies in *KRAS* mutant CRCs, as combined iEGFR plus MI treatment synergistically killed CRCs regardless of *KRAS* status. Future studies could also explore the use of MIs to augment the response to iEGFRs in non-small cell lung cancer, where iEGFRs are regularly used as therapy. Additionally, MIs may have utility in enhancing the efficacy of other therapies that increase cytosolic calcium levels, such as in prostate cancer, where recent work explored the use of selectively targeted thapsigargin analogs (48).

Collectively, our findings are consistent with a model whereby overexpressed menin in CRC cells maintains SKP2 expression, which is important for CRC growth and survival, by increasing active histone marks (H3K4me3) through recruitment of the H3K4 methyltransferase and known menin binding partner MLL (Fig. 7E). When menin is dually inhibited, through direct inhibitors and through increases in cytoplasmic calcium induced by EGFR-independent effects of iEGFRs, *SKP2* transcription is markedly reduced, leading to synergistically reduced cell viability. While we cannot completely rule out that a SKP2-independent process is also involved in this synergy, these results do add to the growing tissue-specific functions of menin, and demonstrate that calcium levels may play an important role in menin-mediated involvement in transcriptional regulation. These data also illustrate the synergy of combined MIs and iEGFRs in suppressing CRC cells, paving the way for the development of new treatment paradigms for CRC.

Supplementary Material

Refer to Web version on PubMed Central for supplementary material.

Acknowledgments

We would like to thank Dr. John Tobias at the University of Pennsylvania Bioinformatics Core for his assistance with the bioinformatics analysis.

Funding: We would like to acknowledge the following support: NIH/NIDDK K08DK106489 (BWK) and R01DK569234 (XH), NIH/NCI R01NCI563378 (XH), the Institute for Translational Medicine and Therapeutics (ITMAT014001) (XH), the Pew Scholars Program in Biomedical Science Award (#50359) (CID, DCB), and the NIH/NIDDK Center for Molecular Studies in Digestive and Liver Diseases at the University of Pennsylvania (P30DK050306) including its pilot grant funding (BWK) and its core facilities (molecular pathology and imaging, and cell culture). The research was also in part supported by the 2016 Neuroendocrine Tumor Research Foundation-AACR Grant, Grant Number 16-60-33-HUA, awarded to Dr. Xianxin Hua (ZF, XH).

References

1. Li JWY, Hua X, Reidy-Lagunes D, Untch BR. MENIN loss as a tissue-specific driver of tumorigenesis. Mol Cell Endocrinol 2017 doi 10.1016/j.mce.2017.09.032.
2. Feng Z, Ma J, Hua X. Epigenetic regulation by the menin pathway. Endocr Relat Cancer 2017;24(10):T147–T59 doi 10.1530/ERC-17-0298. [PubMed: 28811300]

3. Malik R, Khan AP, Asangani IA, Cieslik M, Prensner JR, Wang X, et al. Targeting the MLL complex in castration-resistant prostate cancer. Nat Med 2015;21(4):344–52 doi 10.1038/nm.3830. [PubMed: 25822367]

4. Siegel RL, Miller KD, Jemal A. Cancer Statistics, 2017. CA Cancer J Clin 2017;67(1):7–30 doi 10.3322/caac.21387. [PubMed: 28055103]

5. Cancer Genome Atlas N Comprehensive molecular characterization of human colon and rectal cancer. Nature 2012;487(7407):330–7 doi 10.1038/nature11252. [PubMed: 22810696]

6. Guinney J, Dienstmann R, Wang X, de Reynies A, Schlicker A, Soneson C, et al. The consensus molecular subtypes of colorectal cancer. Nat Med 2015;21(11):1350–6 doi 10.1038/nm.3967. [PubMed: 26457759]

7. Bochis OV, Irimie A, Pichler M, Berindan-Neagoe I. The role of Skp2 and its substrate CDKN1B (p27) in colorectal cancer. J Gastrointestin Liver Dis 2015;24(2):225–34 doi 10.15403/jgld.2014.1121.242.skp2. [PubMed: 26114183]

8. Li JQ, Wu F, Masaki T, Kubo A, Fujita J, Dixon DA, et al. Correlation of Skp2 with carcinogenesis, invasion, metastasis, and prognosis in colorectal tumors. Int J Oncol 2004;25(1):87–95. [PubMed: 15201993]

9. Shapira M, Ben-Izhak O, Linn S, Futerman B, Minkov I, Hershko DD. The prognostic impact of the ubiquitin ligase subunits Skp2 and Cks1 in colorectal carcinoma. Cancer 2005;103(7):1336–46 doi 10.1002/cncr.20917. [PubMed: 15717322]

10. Siegel RL, Miller KD, Fedewa SA, Ahnen DJ, Meester RGS, Barzi A, et al. Colorectal cancer statistics, 2017. CA Cancer J Clin 2017;67(3):177–93 doi 10.3322/caac.21395. [PubMed: 28248415]

11. National Comprehensive Cancer Network. Clinical Practice Guidelines in Oncology: Colon Cancer. Version 1.2018. Accessed 2/16/2018.

12. Wee P, Wang Z. Epidermal Growth Factor Receptor Cell Proliferation Signaling Pathways. Cancers (Basel) 2017;9(5) doi 10.3390/cancers9050052.

13. Maemondo M, Inoue A, Kobayashi K, Sugawara S, Oizumi S, Isobe H, et al. Gefitinib or chemotherapy for non-small-cell lung cancer with mutated EGFR. N Engl J Med 2010;362(25):2380–8 doi 10.1056/NEJMoa0909530. [PubMed: 20573926]

14. Van Cutsem E, Kohne CH, Hitre E, Zaluski J, Chang Chien CR, Makhson A, et al. Cetuximab and chemotherapy as initial treatment for metastatic colorectal cancer. N Engl J Med 2009;360(14):1408–17 doi 10.1056/NEJMoa0805019. [PubMed: 19339720]

15. Mackenzie MJ, Hirte HW, Glenwood G, Jean M, Goel R, Major PP, et al. A phase II trial of ZD1839 (Iressa) 750 mg per day, an oral epidermal growth factor receptor-tyrosine kinase inhibitor, in patients with metastatic colorectal cancer. Invest New Drugs 2005;23(2):165–70 doi 10.1007/s10637-005-5862-9. [PubMed: 15744593]

16. Townsley CA, Major P, Siu LL, Dancey J, Chen E, Pond GR, et al. Phase II study of erlotinib (OSI-774) in patients with metastatic colorectal cancer. Br J Cancer 2006;94(8):1136–43 doi 10.1038/sj.bjc.6603055. [PubMed: 16570047]

17. Kindler HL, Friberg G, Skoog L, Wade-Oliver K, Vokes EE. Phase I/II trial of gefitinib and oxaliplatin in patients with advanced colorectal cancer. Am J Clin Oncol 2005;28(4):340–4. [PubMed: 16062074]

18. Weickhardt AJ, Price TJ, Chong G, Gebski V, Pavlakis N, Johns TG, et al. Dual targeting of the epidermal growth factor receptor using the combination of cetuximab and erlotinib: preclinical evaluation and results of the phase II DUX study in chemotherapy-refractory, advanced colorectal cancer. J Clin Oncol 2012;30(13):1505–12 doi 10.1200/JCO.2011.38.6599. [PubMed: 22412142]

19. Verma N, Rai AK, Kaushik V, Brunnert D, Chahar KR, Pandey J, et al. Identification of gefitinib off-targets using a structure-based systems biology approach; their validation with reverse docking and retrospective data mining. Sci Rep 2016;6:33949 doi 10.1038/srep33949. [PubMed: 27653775]

20. Brehmer D, Greff Z, Godl K, Blencke S, Kurtenbach A, Weber M, et al. Cellular targets of gefitinib. Cancer Res 2005;65(2):379–82. [PubMed: 15695376]

21. Yamamoto N, Honma M, Suzuki H. Off-target serine/threonine kinase 10 inhibition by erlotinib enhances lymphocytic activity leading to severe skin disorders. Mol Pharmacol 2011;80(3):466–75 doi 10.1124/mol.110.070862. [PubMed: 21606217]
22. Hong S, Gu Y, Gao Z, Guo L, Guo W, Wu X, et al. EGFR inhibitor-driven endoplasmic reticulum stress-mediated injury on intestinal epithelial cells. Life Sci 2014;119(1–2):28–33 doi 10.1016/j.lfs.2014.10.008. [PubMed: 25445223]
23. Marchi S, Patergnani S, Missiroli S, Morciano G, Rimessi A, Wieckowski MR, et al. Mitochondrial and endoplasmic reticulum calcium homeostasis and cell death. Cell Calcium 2018;69:62–72 doi 10.1016/j.ceca.2017.05.003. [PubMed: 28515000]
24. Carloni S, Fabbri F, Brigliadori G, Ulivi P, Silvestrini R, Amadori D, et al. Tyrosine kinase inhibitors gefitinib, lapatinib and sorafenib induce rapid functional alterations in breast cancer cells. Curr Cancer Drug Targets 2010;10(4):422–31. [PubMed: 20384581]
25. Team RC. R: A language and environment for statistical computing. Vienna, Austria: R Foundation for Statistical Computing; 2014.
26. Love MI, Huber W, Anders S. Moderated estimation of fold change and dispersion for RNA-seq data with DESeq2. Genome Biol 2014;15(12):550 doi 10.1186/s13059-014-0550-8. [PubMed: 25516281]
27. Huang J, Gurung B, Wan B, Matkar S, Veniaminova NA, Wan K, et al. The same pocket in menin binds both MLL and JUND but has opposite effects on transcription. Nature 2012;482(7386):542–6 doi 10.1038/nature10806. [PubMed: 22327296]
28. Niesen FH, Berglund H, Vedadi M. The use of differential scanning fluorimetry to detect ligand interactions that promote protein stability. Nat Protoc 2007;2(9):2212–21 doi 10.1038/nprot.2007.321. [PubMed: 17853878]
29. Shi A, Murai MJ, He S, Lund G, Hartley T, Purohit T, et al. Structural insights into inhibition of the bivalent menin-MLL interaction by small molecules in leukemia. Blood 2012;120(23):4461–9 doi 10.1182/blood-2012-05-429274. [PubMed: 22936661]
30. Borkin D, He S, Miao H, Kempinska K, Pollock J, Chase J, et al. Pharmacologic inhibition of the Menin-MLL interaction blocks progression of MLL leukemia in vivo. Cancer Cell 2015;27(4):589–602 doi 10.1016/j.ccell.2015.02.016. [PubMed: 25817203]
31. Andersen TB, Lopez CQ, Manczak T, Martinez K, Simonsen HT. Thapsigargin--from Thapsia L. to mipsagargin. Molecules 2015;20(4):6113–27 doi 10.3390/molecules20046113. [PubMed: 25856061]
32. Chen TW, Wardill TJ, Sun Y, Pulver SR, Renninger SL, Baohan A, et al. Ultrasensitive fluorescent proteins for imaging neuronal activity. Nature 2013;499(7458):295–300 doi 10.1038/nature12354. [PubMed: 23868258]
33. Sano K, Voelker DR, Mason RJ. Effect of secretagogues on cytoplasmic free calcium in alveolar type II epithelial cells. Am J Physiol 1987;253(5 Pt 1):C679–86 doi 10.1152/ajpcell.1987.253.5.C679. [PubMed: 2825530]
34. Tymianski M, Spigelman I, Zhang L, Carlen PL, Tator CH, Charlton MP, et al. Mechanism of action and persistence of neuroprotection by cell-permeant Ca2+ chelators. J Cereb Blood Flow Metab 1994;14(6):911–23 doi 10.1038/jcbfm.1994.122. [PubMed: 7929656]
35. Kang SS, Han KS, Ku BM, Lee YK, Hong J, Shin HY, et al. Caffeine-mediated inhibition of calcium release channel inositol 1,4,5-trisphosphate receptor subtype 3 blocks glioblastoma invasion and extends survival. Cancer Res 2010;70(3):1173–83 doi 10.1158/0008-5472.CAN-09-2886. [PubMed: 20103623]
36. Garriga J, Bhattacharya S, Calbo J, Marshall RM, Truongcao M, Haines DS, et al. CDK9 is constitutively expressed throughout the cell cycle, and its steady-state expression is independent of SKP2. Mol Cell Biol 2003;23(15):5165–73. [PubMed: 12861003]
37. Huang H, Regan KM, Wang F, Wang D, Smith DI, van Deursen JM, et al. Skp2 inhibits FOXO1 in tumor suppression through ubiquitin-mediated degradation. Proc Natl Acad Sci U S A 2005;102(5):1649–54 doi 10.1073/pnas.0406789102. [PubMed: 15668399]
38. Reither G, Schaefer M, Lipp P. PKCalpha: a versatile key for decoding the cellular calcium toolkit. J Cell Biol 2006;174(4):521–33 doi 10.1083/jcb.200604033. [PubMed: 16893971]

39. Gstaiger M, Jordan R, Lim M, Catzavelos C, Mestan J, Slingerland J, et al. Skp2 is oncogenic and overexpressed in human cancers. Proc Natl Acad Sci U S A 2001;98(9):5043–8 doi 10.1073/pnas.081474898. [PubMed: 11309491]
40. Lipp P, Thomas D, Berridge MJ, Bootman MD. Nuclear calcium signalling by individual cytoplasmic calcium puffs. EMBO J 1997;16(23):7166–73 doi 10.1093/emboj/16.23.7166. [PubMed: 9384593]
41. Allbritton NL, Oancea E, Kuhn MA, Meyer T. Source of nuclear calcium signals. Proc Natl Acad Sci U S A 1994;91(26):12458–62. [PubMed: 7809059]
42. Baselga J, Rischin D, Ranson M, Calvert H, Raymond E, Kieback DG, et al. Phase I safety, pharmacokinetic, and pharmacodynamic trial of ZD1839, a selective oral epidermal growth factor receptor tyrosine kinase inhibitor, in patients with five selected solid tumor types. J Clin Oncol 2002;20(21):4292–302 doi 10.1200/JCO.2002.03.100. [PubMed: 12409327]
43. McKillop D, Partridge EA, Kemp JV, Spence MP, Kendrew J, Barnett S, et al. Tumor penetration of gefitinib (Iressa), an epidermal growth factor receptor tyrosine kinase inhibitor. Mol Cancer Ther 2005;4(4):641–9 doi 10.1158/1535-7163.MCT-04-0329. [PubMed: 15827338]
44. Zannetti A, Iommelli F, Fonti R, Papaccioli A, Sommella J, Lettieri A, et al. Gefitinib induction of in vivo detectable signals by Bcl-2/Bcl-xL modulation of inositol trisphosphate receptor type 3. Clin Cancer Res 2008;14(16):5209–19 doi 10.1158/1078-0432.CCR-08-0374. [PubMed: 18698039]
45. Yu W, Lu W, Chen G, Cheng F, Su H, Chen Y, et al. Inhibition of histone deacetylases sensitizes EGF receptor-TK inhibitor-resistant non-small-cell lung cancer cells to erlotinib in vitro and in vivo. Br J Pharmacol 2017;174(20):3608–22 doi 10.1111/bph.13961. [PubMed: 28749535]
46. Abdelfatah E, Kerner Z, Nanda N, Ahuja N. Epigenetic therapy in gastrointestinal cancer: the right combination. Therap Adv Gastroenterol 2016;9(4):560–79 doi 10.1177/1756283X16644247.
47. Eckschlager T, Plch J, Stiborova M, Hrabeta J. Histone Deacetylase Inhibitors as Anticancer Drugs. Int J Mol Sci 2017;18(7) doi 10.3390/ijms18071414.
48. Doan NT, Paulsen ES, Sehgal P, Moller JV, Nissen P, Denmeade SR, et al. Targeting thapsigargin towards tumors. Steroids 2015;97:2–7 doi 10.1016/j.steroids.2014.07.009. [PubMed: 25065587]

Statement of Significance

Menin is a calcium-responsive regulator of SKP2 expression, and combining menin inhibition with EGFR-independent cytosolic calcium increases induced by small molecule EGFR inhibitors, synergistically reduces SKP2 expression and suppresses colorectal cancer.

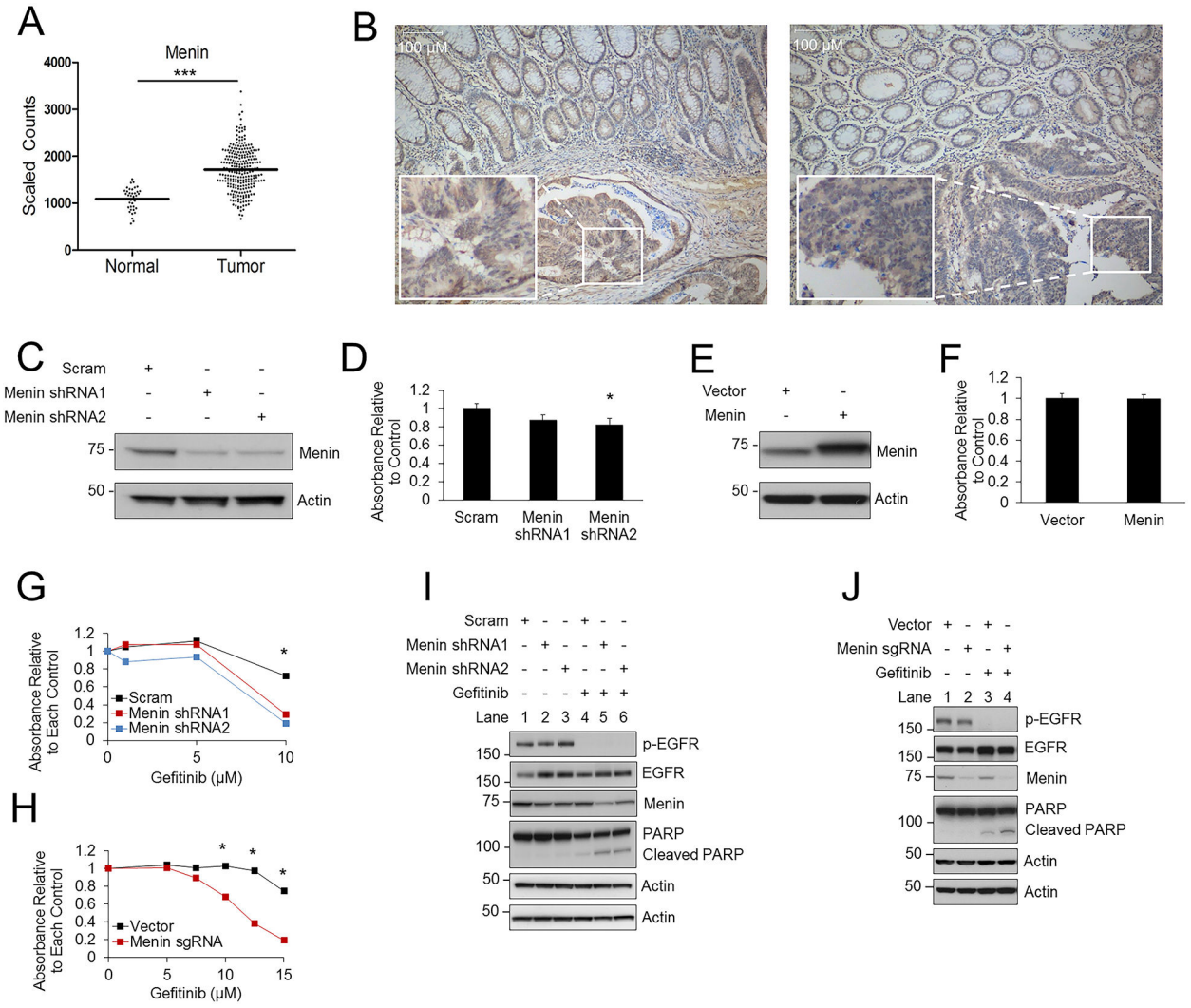

Figure 1: Menin is upregulated in colon cancer and provides resistance to gefitinib.

A) TCGA database analysis comparing menin expression in non-cancerous colonic epithelial samples compared to colon cancer samples. Log2-transformed, normalized counts are shown for menin, dividing the plot to separate normal and tumor samples. *** p = 3.31E-14. B) Menin IHC in colon cancer and adjacent normal colonic mucosa, with two representative examples shown, 100X magnification. C-D) HT-29 cells transduced with either scrambled or menin shRNAs (C), then cell growth was assessed after 96 hours by the MTS assay (D). E-F) HT-29 cells transduced with either vector or menin (E), then cell growth was assessed after 96 hours by the MTS assay (F). G) HT-29 cells transduced with either scrambled or menin shRNAs, then treated with varying concentrations of gefitinib. Cell growth was assessed after 96 hours by the MTS assay. H) HT-29 cells transduced with either lentiCRISPRv2 vector or menin sgRNA, then treated with varying concentrations of gefitinib. Cell growth was assessed after 96 hours by the MTS assay. I) HT-29 cells transduced with scrambled or menin shRNAs, then protein levels were assessed by western blot after 96 hours. 10 μM gefitinib. J) HT-29 cells transduced with either lentiCRISPRv2

vector or menin sgRNA, then protein levels were assessed by western blot after 96 hours. 10 μM gefitinib. * $p < 0.05$.

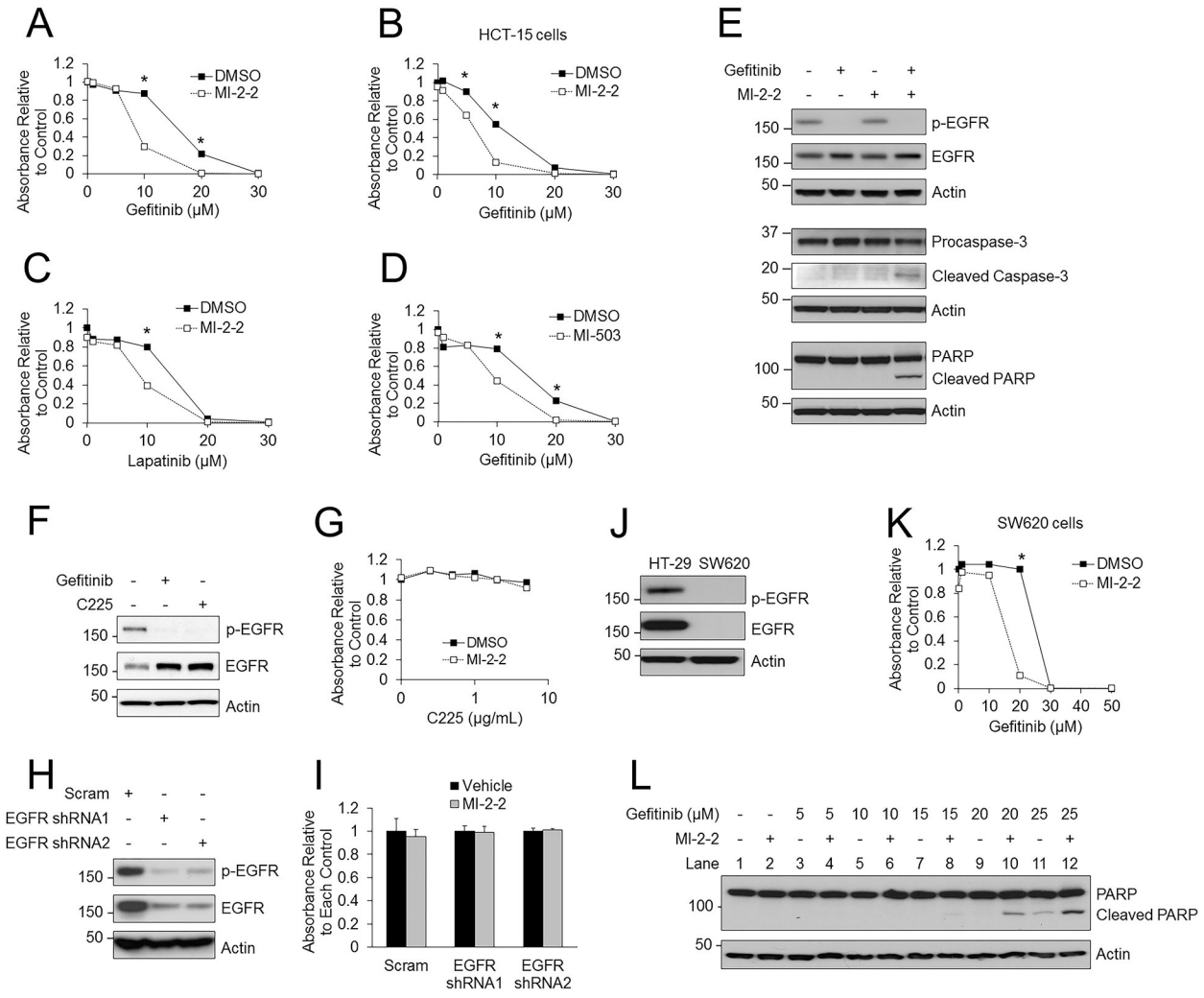

Figure 2: Menin inhibition sensitizes colon cancer cells to iEGFRs in an EGFR-independent manner.

A) Treatment of HT-29 cells with various concentrations of gefitinib, with and without 1 μM MI-2–2, with cell growth assessed after 96 hours by the MTS assay. B) HCT-15 cells treated with varying concentrations of gefitinib with and without 1 μM MI-2–2. MTS assay performed after 96 hours. C) HT-29 cells treated with varying concentrations of lapatinib with and without 1 μM MI-2–2. MTS assay performed after 96 hours. D) HT-29 cells treated with varying concentrations of gefitinib with and without 1 μM MI-503. MTS assay performed after 96 hours. E) HT-29 cells treated for 96 hours followed by analysis of protein levels by western blotting, 10 μM gefitinib, 1 μM MI-2–2. F) HT-29 cells treated for 96 hours and then analyzed by western blotting. 10 μM gefitinib, 1 μg/mL C225. G) HT-29 cells treated with varying concentrations of C225 with or without 1 μM MI-2–2 for 96 hours, and then cell growth was assessed by the MTS assay. H) HT-29 cells transduced with scrambled or EGFR shRNAs, with EGFR protein expression analyzed by western blot. I) Scrambled and EGFR shRNA transduced HT-29 cells were treated with vehicle or 1 μM MI-2–2 for 96 hours, and then cell growth was assessed by the MTS assay. J) EGFR expression was assessed by western blotting in HT-29 and SW620 cells. K) SW620 cells

treated with varying concentrations of gefitinib with and without 1 μM MI-2–2. MTS assay was performed after 96 hours to assess cell growth. L) SW620 cells treated with varying concentrations of gefitinib with and without 1 μM MI-2–2 for 96 hours, then protein levels were analyzed by western blotting. * $p < 0.05$.

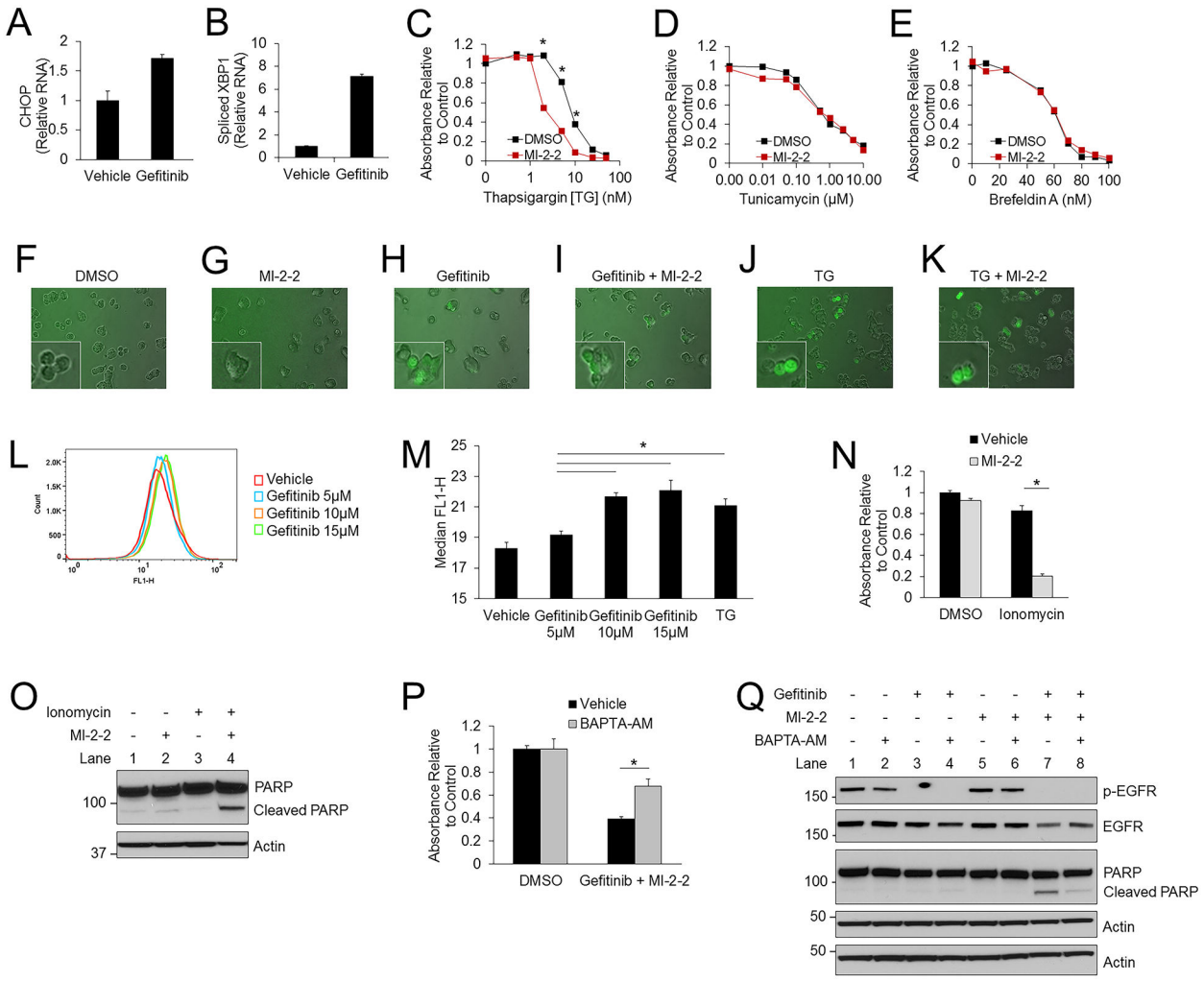

Figure 3: Increased cytosolic calcium is important for gefitinib mediated suppression of CRC cells.

A-B) HT-29 cells treated for 48 hours and then CHOP mRNA (A) and spliced XBP1 mRNA (B) were assessed by RT-PCR and plotted relative to actin. 10 μM gefitinib. C-E) HT-29 cells treated with varying concentrations of thapsigargin [TG] (C), tunicamycin (D), and brefeldin A (E), with and without 1 μM MI-2–2. Cell growth was assessed after 96 hours by the MTS assay. F-K) HT-29-GCaMP6f cells treated for 24 hours. Images were obtained at 200X. 1 μM MI-2–2, 10 μM gefitinib, 2 nM TG. L-M) HT-29-GCaMP6f cells treated with either gefitinib (L) or 2nM TG for 72 hours and then cytosolic calcium levels were analyzed by flow cytometry, with the median FLH-1 values reported (M). N) HT-29 cells treated for 96 hours with cell growth assessed by the MTS assay. 10 μM ionomycin, 1 μM MI-2–2. O) HT-29 cells treated for 96 hours, with protein analyzed by western blot. 5 μM ionomycin, 1 μM MI-2–2. P-Q) HT-29 cells treated for 96 hours with cell growth assessed by the MTS assay (P), and treated for 48 hours with protein analysis by western blot (Q). 10 μM gefitinib, 1 μM MI-2–2, 5 μM BAPTA-AM. * $p < 0.05$.

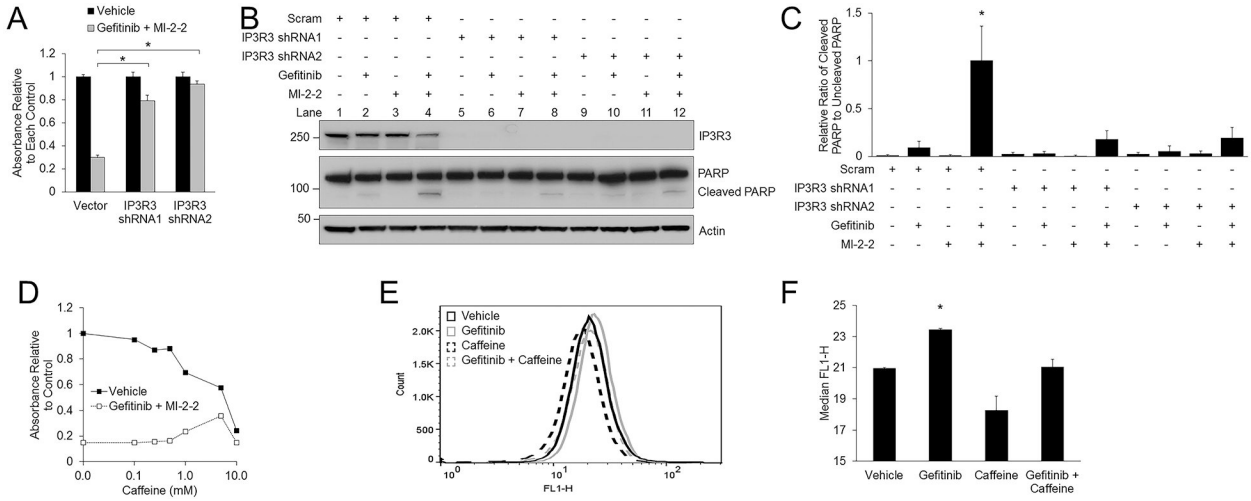

Figure 4: Gefitinib induces CRC repression through activation of IP3R3.

A-B) HT-29 cells transduced with either scrambled or IP3R3 shRNAs, then treated with vehicle or 10 μM gefitinib/1 μM MI-2–2. Cell growth was assessed after 96 hours by the MTS assay (A) and protein levels were assessed after 48 hours by western blot (B). C) Quantitation and normalization of cleaved and uncleaved PARP levels on western blot from Figure 4B. D) HT-29 cells treated with vehicle or 10 μM gefitinib/1 μM MI-2–2 with different concentrations of caffeine for 96 hours with cell growth assessed by the MTS assay. E-F) HT-29-GCaMP6f cells treated for 24 hours with cytosolic calcium levels analyzed by flow cytometry (E), with the median FLH-1 values reported (F). 10 μM gefitinib, 2 mM caffeine. *$p < 0.05$.

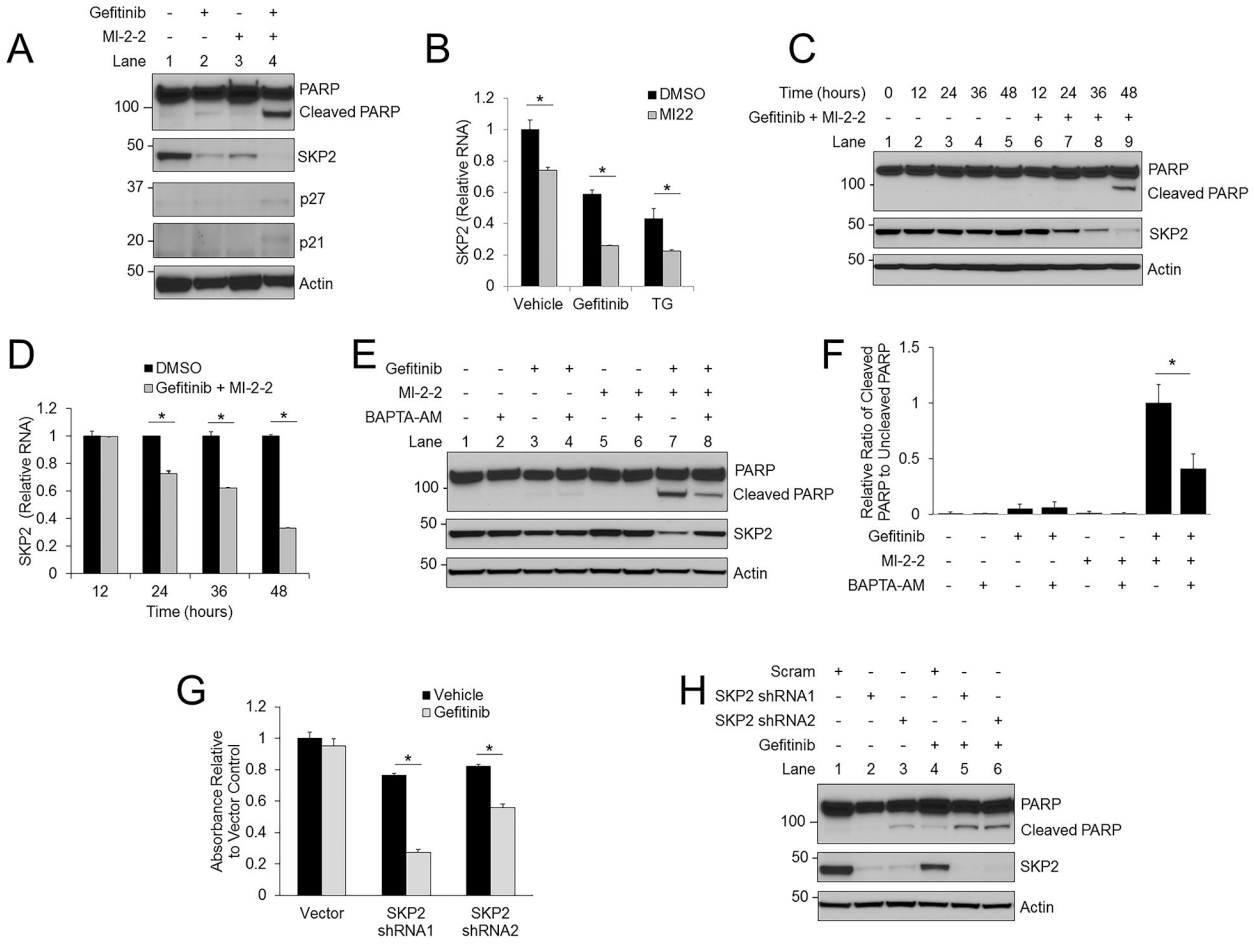

Figure 5: Gefitinib and menin inhibition synergistically decrease SKP2 expression in a calcium-dependent manner.

A) HT-29 cells treated for 48 hours followed by analysis of protein levels by western blotting. 10 μM gefitinib, 1 μM MI-2–2. B) After 48 hours of treatment in HT-29 cells SKP2 mRNA was assessed by RT-PCR and plotted relative to actin. 1 μM MI-2–2,10 μM gefitinib, 5 nM TG. C-D) A time course was performed in HT-29 cells treated with either vehicle or 10 μM gefitinib/1 μM MI-2–2, with analysis of protein levels by western blotting (C) and SKP2 mRNA assessment by RT-PCR, plotted relative to actin, and normalized to DMSO for each time point (D). E) HT-29 cells treated for 48 hours with protein analysis by western blot. 10 μM gefitinib, 1 μM MI-2–2, 5 μM BAPTA-AM. F) Quantitation and normalization of cleaved and uncleaved PARP levels on western blot from Figure 5E. G-H) HT-29 cells transduced with either scrambled or SKP2 shRNAs, then treated with 10 μM gefitinib. After 96 hours, cell growth was assessed by the MTS assay (G) and after 48 hours protein levels were assessed by western blot (H). * $p < 0.05$.

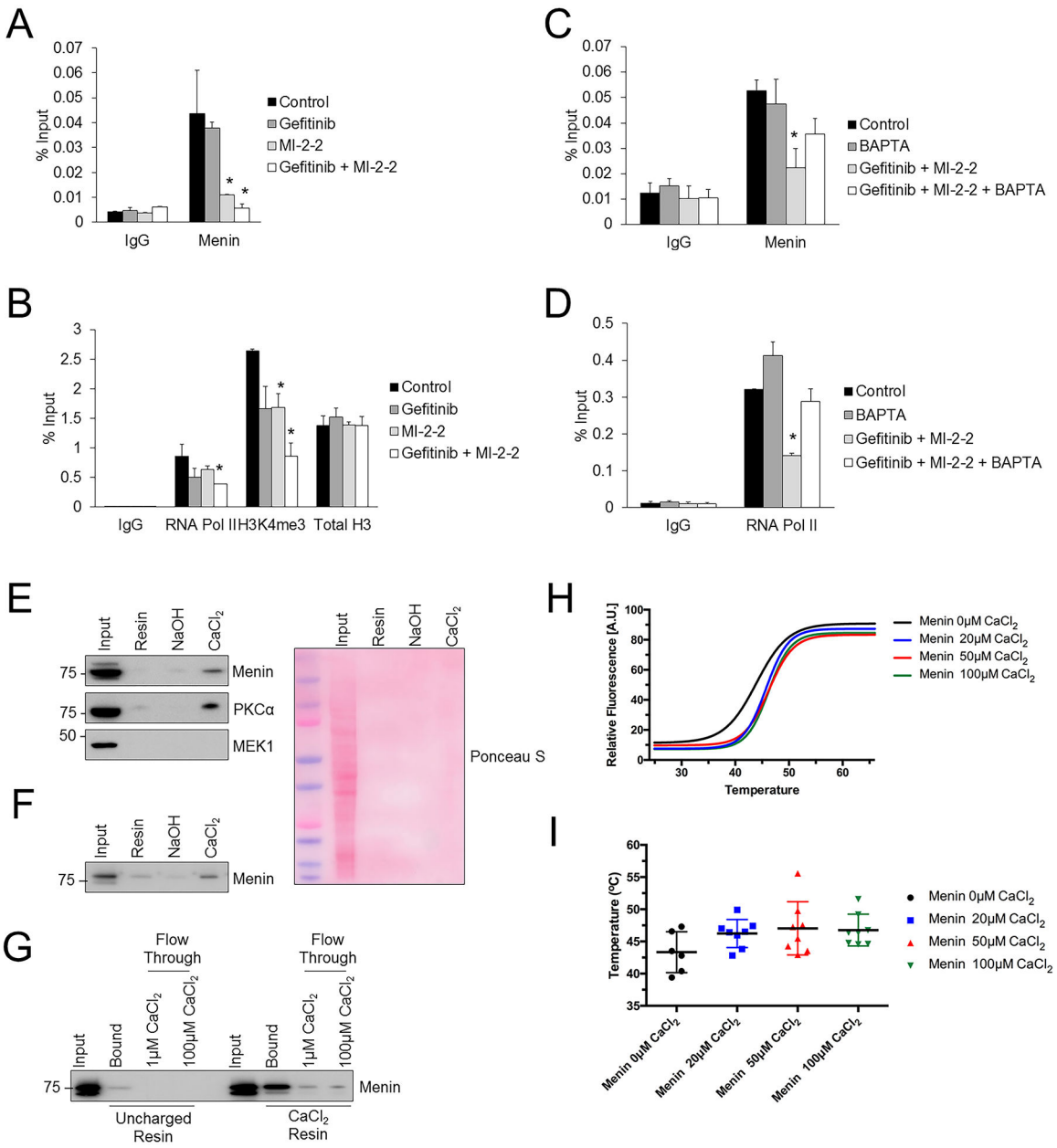

Figure 6: Menin interacts directly with calcium and regulates the levels of active histone marks and SKP2 transcription.

A-B) HT-29 cells were treated for 30 hours, then ChIP assay was performed to look for menin (A), RNA polymerase II, H3K4me3, and total H3 (B) at amplicon 1 of the SKP2 promoter. 10 μM gefitinib, 1 μM MI-2–2. *p < 0.05 compared to Control. C-D) HT-29 cells were treated for 30 hours, then ChIP assay was performed to look for menin (C) and RNA polymerase II (D) at amplicon 1 of the SKP2 promoter. 10 μM gefitinib, 1 μM MI-2–2, 2 μM BAPTA-AM. *p < 0.05 compared to Control and BAPTA-AM. E) Chelex resin eluent after incubation with HT-29 cell lysate. Uncharged resin or resin prepared with NaOH or $CaCl_2$. Equal volumes of eluent were utilized to analyze protein by western blot. Ponceau S demonstrated no significant non-specific protein binding to resin. F) Chelex resin eluent

after incubation with purified recombinant menin protein. Uncharged resin or resin prepared with NaOH or $CaCl_2$. Equal volumes of eluent were utilized to analyze protein by western blot. G) After incubation with recombinant menin protein, uncharged and $CaCl_2$ Chelex resin was washed with different calcium concentrations with resulting protein eluent examined by western blot. H-I) Differential scanning fluorimetry was performed on purified recombinant menin protein with different concentrations of $CaCl_2$, with example fitted curves (H) and average melting temperatures (I).

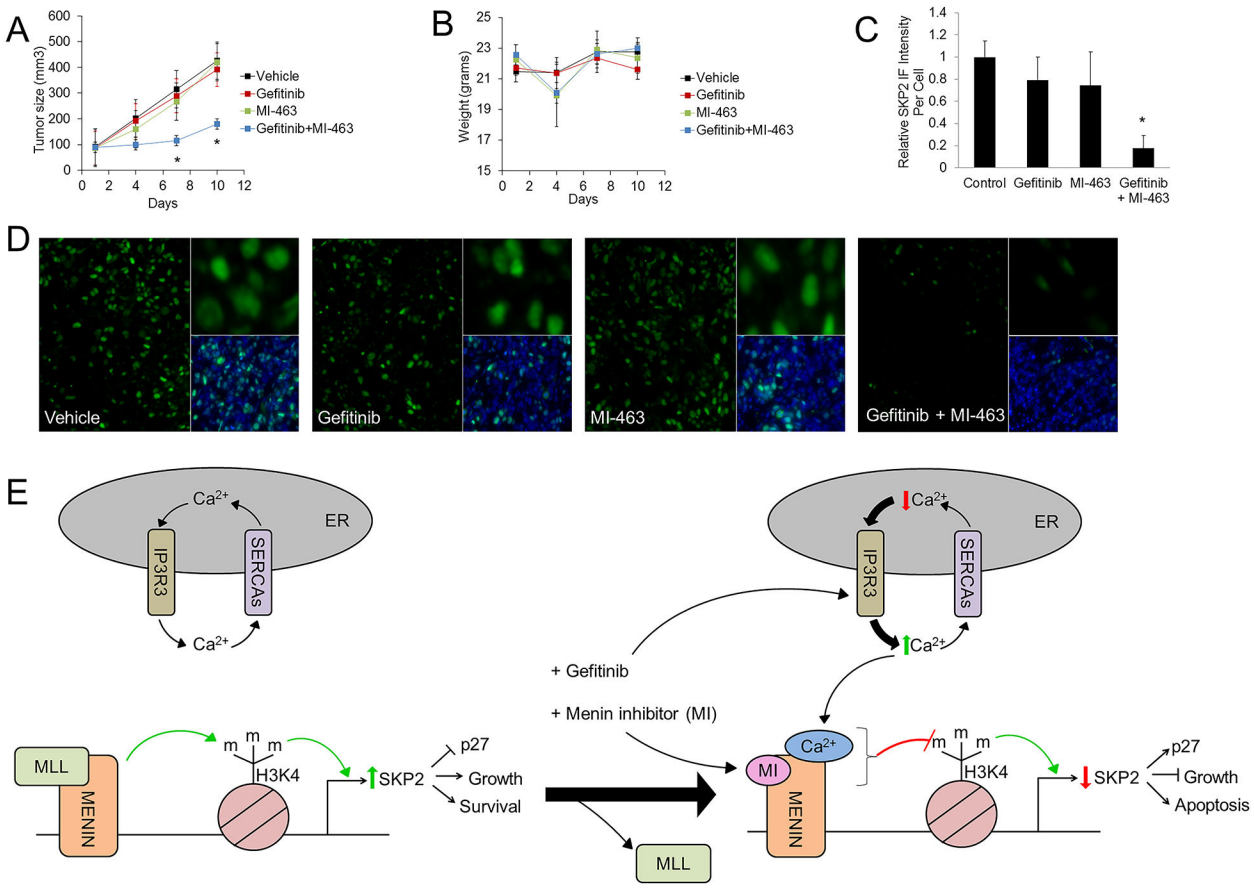

Figure 7: Combined menin inhibition and gefitinib reduces colon cancer xenograft growth and suppresses SKP2.

Nude mice were transplanted with HT-29 cells, and once tumor size reached approximately 100mm^3, treatment was started with either gefitinib (100 mg/kg daily by oral gavage), MI-463 (35 mg/kg daily by IP/SQ injection), the combination of gefitinib plus MI-463, or vehicle control. A) Tumor size was measured with a Vernier caliber every 3 days. Error bars indicate +/− SEM. B) Mice were weighed every 3 days. Error bars indicate +/− SD. C-D) SKP2 immunofluorescence was performed in the xenografts with quantitation of SKP2 immunofluorescence (C) and representative images from each of the 4 treatment groups (D). E) A representative model of menin and iEGFR involvement in SKP2 regulation. * $p < 0.05$.